

Transport properties of Valine in water at different temperatures

Deepak Pandey and Narayan Prasad Adhikari*

Central Department of Physics, Tribhuvan University, Kirtipur, Kathmandu, Nepal

Molecular Dynamics simulations of Valine in water and their binary mixtures ($N_{Val} = 0.003$ & $N_{water} = 0.997$, N representing the mole fraction) have been accomplished at temperatures 293.20 K, 303.20 K, 313.20 K, 323.20 K, and 333.20 K using the OPLS/AA force field parameters. The work has been carried out by using GROMACS. The OW-OW, H19-OW, N6-OW and C1/C3-OW radial distribution functions (RDFs) have been estimated. Co-ordination numbers are also determined by the self-coded FORTRAN. The self-diffusion coefficients of Valine and water have been determined by means of mean-square displacement (MSD) using Einstein's relation. The mutual diffusion coefficients of the binary mixtures have been determined using Darken's relation. The values of the diffusion coefficients have been found to agree with the experimental results within 8.54 %. The temperature dependence of the diffusion coefficients have been analyzed and the analysis showed that they follow Arrhenius behavior. Energy estimated from Arrhenius plot agrees with experimental data within 13.04 % for water and 5.34 % for system.

Keywords: Valine, Diffusion Coefficient, Radial distribution function (RDF), Mean square displacement (MSD), Molecular dynamics (MD), Arrhenius behavior

INTRODUCTION

The amino acid contains both amine ($-NH_2$) and carboxylic acid ($-COOH$) as its functional groups. Amino acid helps to make protein which is composed of C, O, N and H atoms. There exist twenty standard amino acids, out of them, nine are known as essential (indispensable) and rest are non-essential (dispensable). The essential amino acids can't be produced by our human body¹. Twenty different L- α -amino acids can build different sort of proteins, which include a linear polymer, where all the proteinogenic amino acids manifest mutual structural features with both α -carbon to the amino group, a carboxylic acid group. Amino acids can be classified also into polar (hydrophilic) and non-polar (hydrophobic)¹.

Valine is symbolized by Val. It is obtained by hydrolysis of protein. It is aliphatic R-group, long branched-chain amino acid (BCAA) and an essential (indispensable) amino acid which easily pairs with another BCCA (leucine, and isoleucine). Plants are the main source of essential amino acids. It is also known as *2-amino-3-methyl butanoic acid*. It is a precursor in the penicillin bio-synthesis of proteins pathway². It is expected to be found the interior of the protein. Val is known as aliphatic, hydrophobic amino acid. Its molecular formula is $C_5H_{11}NO_2$. Its molar mass is 117.148 g/mol, and the melting point is $315^\circ C$ ³.

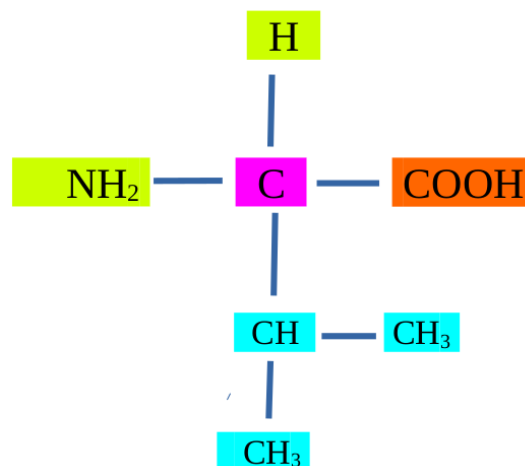


FIG. 1. Molecular formula of Valine.

FIG.1 shows a Val molecule. It contains α -amino group (left side), an α -carboxylic group (right side) and methyl chain as (lower part), Val in this structure contains two non-hydrogen part to C-beta carbon. It is bulkiness near to protein backbone, which streaks to adopt main-chain and an alpha-helical conformation; it lies within beta-sheets easily. It helps to grow, regulate blood sugar, repairs muscles, cells, tissues, maintains the energy of our body as well as stir nervous system, and helps to proper mental functioning (mental vigor) etc. in our body⁴. It inhibits the transport of

Tryptophan to the blood-brain barrier which causes a low level of mood, sleep regulation of serotonin⁵. Val helps to remove toxic (nitrogen) from the liver which enables to transport nitrogen from one tissue of the body to other parts and maintain muscles as well as the regulation of the immune system. The deficiency of Val can cause loss of weight, skin problems, hair loss, sleep disorder, mood swing, erectile disorders, arthritis, diabetes, maple syrup urine disorder, cardiovascular imbalance (high cholesterol level, high blood pressure, menopausal complaints) in human⁶ and legs abnormalities in animals (mainly in chicken)⁷. It performs positive appetite suppressant, insomnia, and nervousness. Val plays a vital role for muscles metabolism, where it assists right amount of Nitrogen in the body which provides stimuli. L-Val and D-Val isomers converted into glucose in the liver is called *Glucogenic amino acid*, which certainly balances emotional calm, and muscles coordination. Val increases insulin secretion from the pancreas within 3–9 % and it boosts glycogen synthesis in the muscle cell. Mostly wrestlers (bodybuilders) use Val with isoleucine and leucine to boost body growth and to regulate the energy⁸. L-Val uptake appears in the cotyledons when their water content has decreased to 65%⁹ as well as the mechanism of amino acid transport in sea urchin embryos possess similarities to the well-described transport system present in mammalian¹⁰. L-Val increases its urinary excretion in rats^{11,12}, the decreasing intestinal transport of L-Val with increasing age/weight in rats¹³. An experimental research has been carried out to calculate the diffusion coefficient of amino acids at the different concentration at 20 °C in water¹⁴. At each temperature diffusion coefficient value decrease with increasing molar mass¹⁵, diffusivity gradually decreases with increasing interactive strength.

Molecular dynamics simulations have been performed to understand the physics behind reaction or extraction process of amino acids in our body, estimation of mass transfer rates is important: diffusion coefficients are one of the most fundamental quantities. Diffusion can provide meaningful information about intermolecular interactions: the translation motion of the molecular diffusion reflects the friction arising from the intermolecular interaction between the surrounding & diffusing molecules¹⁵. It is necessary and important to measure the diffusion coefficients of amino acids from a scientific viewpoint not only an engineering. Despite the experimental estimation of the diffusion process of Valine¹⁵, to the best of our knowledge, there has been no molecular dynamics study on the diffusion of Valine in water at different temperatures.

DIFFUSION

The process of transferring mass from a system having the higher concentration to the region of a system having lower concentration as a result of random molecular motions is called diffusion¹⁶. This phenomenon is chronicled by Thomas Graham “Density especially does not play any role when different nature of gases brought into contact to arrange themselves like heaviest sink down and lighter float up, but they spontaneously diffuse, mutually and equally, through each other, and persist in the pally state of the mixture for any length of time”. The sort of diffusion where no chemical concentration gradient exists in a homogeneous system is called Self-Diffusion. It often occurs when the mixing of identical molecules to the solution overall. The corresponding coefficient is called self-diffusion coefficient. Being the different characters in concentration for the same sort of molecules invites to an equilibrium state, is begotten by random motion. Self-diffusion is characterized due to noncooperative random-walk motion of the individual molecules¹⁷. This diffusion is studied by Mean square displacement (MSD) known as *Einstein relation*¹⁸. In case of three dimensional system, the mean square displacement (MSD) and self-diffusion coefficient can be related by;

$$D = \lim_{t \rightarrow \infty} \frac{\langle [r(t) - r(0)]^2 \rangle}{6t}. \quad (1)$$

In equation 1 the bracket term $[r(t) - r(0)]$ represents change in position of diffusing particles at time t from $t = 0$ and nominator of this equation is ensemble average such that $[r(t) - r(0)]^2$ related with MSD of diffusing particles. When we draw the MSD vs time then we get a straight line then we fit best-fitted line, and slope of this best fitted line gives the value which is equal to the sixth times of diffusion coefficient of that particle at that temperature.

The sort of diffusion which occurs in the binary mixture (two distinct molecules) i.e., the heterogeneous system is known as Binary Diffusion. The corresponding coefficient is called Binary Diffusion coefficient. In various senses, we can call it mutual, chemical, inter transport –Diffusion. The expression for Binary Diffusion coefficient is given by famous Darken’s relation¹⁹,

$$D_{12} = D_1 N_2 + D_2 N_1 \quad (2)$$

where D_{12} is the binary diffusion coefficient. D_1 & D_2 are self-diffusion coefficients of the respective molecules. N_1 & N_2 are the mole fraction of respective molecules. If the mixture is about to infinitesimal then the binary diffusion coefficient is almost equal to the self-diffusion coefficient of one of the constitutive particles (components). The theoretical analysis of binary diffusion is more complex than self-diffusion due to being characterized via cooperative motion¹⁸.

COMPUTATIONAL DETAILS

The classical molecular dynamics (MD) is one of the best computational simulation technique for equilibrium and transport property of many (N) body problems. If positions and velocities of the state of molecules at any instead of time are well known then it seems more predictable. The classical method that refers to the nuclear motion of the integral particles obeys the laws of classical mechanics- this is the brilliant estimation for an extensive sector of materials²⁰. Using MD, Lennard-Jones potential can explain van der Waals interactions which are based on Fritz London theory¹⁸. MD is more similar to the real experiments: what we perform in real experiments we do same.

In MD simulation we can measure an observable quantity-which must be expressed as a function of position and momenta of the particles in the system. The temperature in a classical N -body system, using equipartition of energy overall degrees of freedom that enter quadratically in the Hamiltonian of the system, average K.E. per degree of freedom,

$$\langle \frac{1}{2}mv_\alpha^2 \rangle = \frac{1}{2}k_B T. \quad (3)$$

We solve Newton's equation for individual interacting (i^{th}) particles i.e.,

$$m_i \dot{\mathbf{v}} = -\nabla_i U(\mathbf{r}_i) = \mathbf{F}_i, \quad \dot{\mathbf{v}} = \frac{\partial^2 \mathbf{r}_i}{\partial t^2} \quad (4)$$

here, m_i is the mass, \mathbf{r}_i is the position of the i^{th} particles, $U(\mathbf{r}_i)$ is the average potential experienced by the i^{th} particles and \mathbf{F}_i is the mean force on the particle.

We start molecular dynamics process by modeling system which consists of specified molecules as atomic masses, charges, van der Waals radii, force field and more. This model contains the topology-consists of atoms, which are connected to each other

& resembles with the real system. Atoms experience a force from its pairwise additive interaction with other systems. The total potential energy is linear contributions of bonded and non-bonded interactions²¹;

$$U_{total} = \underbrace{(U_{bond} + U_{angle} + U_{dihed})}_{\text{bonded potentials}} + \underbrace{(U_{vdW} + U_{Coulomb})}_{\text{non-bonded interaction}} \quad (5)$$

Then, we specify the initial positions and velocities to all molecules in our input file (*val.pdb*) which enables to create a trajectory of the particle in the phase space. Velocities are created randomly and rescaled to match the constrained temperature. Different interactions are responsible for force experience by individual atoms. Force in each particle is calculated in each step and trajectory is created in accordance. Using Maxwell-Boltzmann distribution, we can find the position and velocity of each particle and integrate Newton's equation of motion with leapfrog algorithm.

Simulation Set Up

Simulation was carried out for Val-water system at a different temperatures. Val ($C_5H_{11}N_2$) is electrically neutral, it contains an amine group (NH_2) and a carboxyl group ($COOH$) covalently bonded with C4. The 4 C -atoms are also covalently bonded as C-C-C-C. Because of the difference in electro-negativity, different atoms in this molecule have different partial charges. The structure of Val molecule depends strongly in the pH of the medium and takes neutral form. Bonds, bond angles, and proper dihedral characterizes its (Val's) topology and electrostatic properties are led by the partial charges and van der Waals interactions are controlled by defining LJ parameters. All the bonded and non-bonded interactions are taken into account in our model to make the Val as real as possible. While modeling this, we have taken all atoms model so all atoms are characterized individually. OPLS/AA *oplsaa.ff* force field is used to optimize all interactions in the GROMACS package. Necessary information about the bond structures with respective *opls-code* and charges are saved in the file *aminoacids.rtp* as well as atoms types and their respective masses are elucidated in *atomtypes.atp*. We use *nrexcl 3* to exclude non-bonded interaction in nearest three bonded neighbor.

We have used the SPC/E water model. It accounts for the best values of the bulk water dynamics structure. It has the high value of dipole moment around 2.35 D and we know charge models are constant this correctly adds 1.25 kcal/mol to the total energy. This model results in better density and diffusion constant than SPC model. It gives accurate tetrahedral angle 109.49° where other models give 104.52° . This model consists of 3 point

charges on each atomic site, one oxygen atom pair with two hydrogen atoms (HW1–OW–HW2). Although the water molecule is electrically neutral, each atom carries partial charges where each hydrogen atom carries a partial charge of +0.4238e, and oxygen atom carries a partial charge of -0.8476e. Here, $e = 1.6022 \times 10^{-19}$ C is the elementary charge²². In GROMACS, the file *spce.itp* contains all these parameters. The force field parameters for the rigid SPC/E model are presented below:

TABLE I. Force field parameters for SPC/E water model.

Parameters	Values
K_{OH}	3.45×10^5 kJ mol ⁻¹ nm ⁻²
b_{OH}	0.1 nm
K_{HOH}	3.83×10^2 kJ mol ⁻¹ rad ⁻²
Θ_o	109.47°

The information about the non-bonded parameters are explained in file *ffnonbonded.itp* follows;

[atomtypes]							
name	at.num	mass	charge	ptype	sigma (σ)	epsilon (ϵ)	
C7	6	12.01100	0.520	A	3.75000e-01	4.39320e-01	
O9	8	15.99940	-0.440	A	2.96000e-01	8.78640e-01	
O8	8	15.99940	-0.530	A	3.00000e-01	7.11280e-01	
H19	1	1.00800	0.450	A	0.00000e+00	0.00000e+00	
N6	7	14.00670	-0.900	A	3.30000e-01	7.11280e-01	
H18	1	1.00800	0.360	A	0.00000e+00	0.00000e+00	
H17	1	1.00800	0.360	A	0.00000e+00	0.00000e+00	
C4	6	12.01100	0.120	A	3.50000e-01	2.76144e-01	
H5	1	1.00800	0.060	A	2.50000e-01	6.27600e-02	
C2	6	12.01100	-0.060	A	3.50000e-01	2.76144e-01	
H13	1	1.00800	0.060	A	2.50000e-01	1.25520e-01	
C3	6	12.01100	-0.180	A	3.50000e-01	2.76144e-01	
H10	1	1.00800	0.060	A	2.50000e-01	1.25520e-01	
H11	1	1.00800	0.060	A	2.50000e-01	1.25520e-01	
H12	1	1.00800	0.060	A	2.50000e-01	1.25520e-01	
C1	6	12.01100	-0.180	A	3.50000e-01	2.76144e-01	
H14	1	1.00800	0.060	A	2.50000e-01	1.25520e-01	
H15	1	1.00800	0.060	A	2.50000e-01	1.25520e-01	
H16	1	1.00800	0.060	A	2.50000e-01	1.25520e-01	
OW	8	15.99940	-0.820	A	3.16557e-01	6.50194e-01	
HW1	1	1.00800	0.410	A	0.00000e+00	0.00000e+00	
HW2	1	1.00800	0.410	A	0.00000e+00	0.00000e+00	

1st column represents the name of corresponding atoms, as well as OW stands for oxygen atom of water, HW1 and HW2 stand for two hydrogen atoms of water molecules. 2nd column notifies the atomic number of respective atoms of our system, 3rd stands for their masses in the atomic unit. 4th column specializes partial charges of atoms of the molecule. 5th column itemizes particle type and A stands for atom. 6th and 7th columns give the value of σ and ϵ of the corresponding atoms. GROMACS does not understand σ and ϵ such that we convert them into the form of C_{ij}^6 and C_{ij}^{12} using;

$$C_{ij}^{(12)} = 4\epsilon_{ij}\sigma_{ij}^{12} \quad \& \quad C_{ij}^{(6)} = 4\epsilon_{ij}\sigma_{ij}^6 \quad (6)$$

The pairs which are involved in the LJ interaction and modified parameters σ_{ij} and ϵ_{ij} can be calculated by Lorentz–Berthelot rules²³;

$$\sigma_{ij} = (\sigma_{ii}\sigma_{jj})^{\frac{1}{2}} \quad \& \quad \epsilon_{ij} = (\epsilon_{ii}\epsilon_{jj})^{\frac{1}{2}} \quad (7)$$

Before solvation, only three molecules of Val are presented in the cubic box of dimension 3 nm × 3 nm × 3 nm. After completion of solvation of Val in water by **genbox** command. Now our system is ready for simulation. Still, the configuration of molecules specified in *afgen.gro* (structure file after solvation) is very far from being an equilibrium: it might contain bad contacts, atoms nearer than van der Waal radius. Forces may be too large and this tends to fail the MD simulation. To succeed in this failure, the process of energy minimization is required which helps to bring our system in the equilibrium state. In order to remove “clashes” i.e., close over ions (LJ core) we perform energy minimization, which reduces the thermal noise in the structures and potential energies so they can be compared better. The steepest-descent algorithm is used as the integrator for em, without fixing any constraints because it moves in the direction parallel to the force (i.e., negative gradient of potential energy function) to reach the minimum; without considering any of the history built in the past. Here, *nsteps* is the maximum number of (minimization) steps to perform for this process. *emtol* = 50 represents the force tolerance in kJ mol⁻¹ nm⁻¹ means it helps to stop minimization when the maximum force < 50 kJ mol⁻¹ nm⁻¹. *emstep* = 0.001 is initial step size for position in nm. *nstcomm*= 1 is the frequency for a center of mass motion removal, *ns_type* = *grid* is to make a grid in the box and only check atoms in neighboring. *rlist*= 1.0 is fixed for cut-off distance for the short-range neighbor list in nm. *coulombtype* = PME is used for the treatment of long-range electrostatic interactions, *vdwtype* = cut-off and *rcoulomb*=1.0 and *rvdw*=1.0 are for Coulomb and van der Waals cut-off. *nstxout* = 200 represents the number of steps that elapse between writing coordinates. In this step, our system is not coupled with thermostat and barostat to maintain temperature and pressure because of fixed box size. *gen-vel* = *no* represents the velocities are set to zero when there are no velocities in the input structure file. FIG.2 represents our system after energy minimization (em); after energy minimization molecules in box remain in more stable than before.

Energy minimization makes our system ready for the MD run. The physical properties of the system in equilibrium are not depended to initial conditions then equilibration run is performed for this. It helps to study dynamical variable which is always altered with different parameters like temperature, pressure, density, etc., in this step system should be coupled to thermostat and barostat. Which helps to bring to the state of thermodynamical equilibrium. Then we perform production run. Thermal equilibrium and constant pressure are obtained by coupling of the system with a suitable thermostat and barostat called temperature and pressure coupling respectively used to rescale their respective parameters.

PME (Particle Mesh Ewald) type is used for long-range

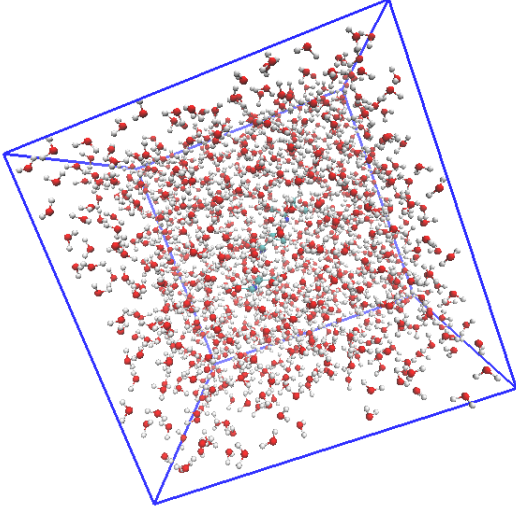


FIG. 2. System under study after energy minimization.

Coulomb interaction with Fourier-spacing of 0.12 nm grid spacing for FFT with cut-off distance of 1.0 nm. $nslist = 10$ is the frequency to update the neighbor list. $ns_type = grid$ is used to search neighboring grid cells in non-bonded interaction within 1.0 nm of reference particle. $v-rescale$ is used for temperature coupling i.e., modified Berendsen thermostat. Different runs are carried out at five different temperatures 293.20 K, 303.20 K, 313.20 K, 323.20 K and 333.20 K. The parameter ref_t is the reference temperature; which, is set according to the different temperature at which simulation carried out. By fixing 0.01 ps time constant for temperature coupling. In similar pattern pressure coupling is also fixed by Berendsen barostat to 1 bar as a reference pressure with the time constant 0.8 ps; for water at 1 atm pressure at 300 K, isothermal compressibility is $4.6 \times 10^{-5} \text{ bar}^{-1}$. Velocities are generated according to Maxwell distribution at different temperatures. During equilibration run, all bonds are converted into constraints using constraint algorithm LINCS.

When the system is equilibrated by the NPT ensemble then we start to production run. After NPT ensemble density, temperature, and pressure of our system are fixed. In this step, we apply NVT ensemble to study diffusion coefficient of Val. The pressure is not needed to couple: we don't use velocity generation because initial velocities are used as what generated in equilibration. LINCS algorithm is used in the production run.

RESULTS AND DISCUSSION

In this section, we discuss the structural properties and diffusion coefficient of the constituents of the systems.

STRUCTURE OF THE SYSTEM

To analyze the structure of our system we do study about radial distribution function (RDF). It gives the ideas about how the atoms or molecules are packed with respect to reference atom or molecule. Structure of the solvent can be interpreted by RDF. It describes how density and probability vary with distance.

Radial Distribution Function of Solvent

Within the preferred simulation box, RDF describes the equilibrium structure of the water molecules. In this simulation, we have taken the SPC/E water model. Hydrogen atoms of water do not take part in LJ interaction with any other atoms. We use RDF g_{OW-OW} to study the structure of water molecule in this simulation.

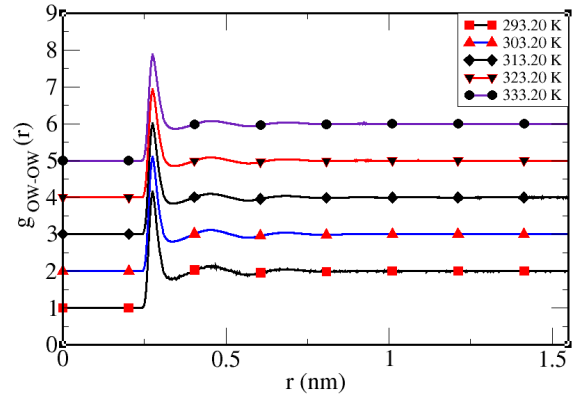


FIG. 3. Plot of the RDF $g_{OW-OW}(r)$ i.e., Oxygen-Oxygen of water molecule vs $r(\text{nm})$ at the different temperature.

In FIG.3, we have drawn different RDF at corresponding temperatures. This gives the probability of finding the oxygen atom of a water molecule at a distance r around the reference oxygen atom of the water molecule. In FIG.3, reference atom is fixed at the origin. First peak point is seen which is very close to the reference oxygen atom. The magnitude of the g_{OW-OW} is zero within atomic separation. Similarly, the second peak does contain the second closest oxygen atoms to reference oxygen atom. Between first and second peak, there is the lowest region around $r \approx 0.334 \text{ nm}$, this notifies that, there is very low probability to find oxygen atoms within this region. These peaks represent coordination shells. As in figure after certain distance i.e., beyond the third peak, the RDF is a straight line and it appears to be 1 means there exists almost no pair correlation. As shown in table II first, second and third peak points and their corresponding values are measured. For example, at 293.20 K first peak point is at 0.2740 nm with corresponding value (height) 3.1514, second peak point at 0.4520 nm with

corresponding value 1.1398 and so on. It means that the closest atoms can be found is at distance 0.2740 nm and it is 3.15 times more possibilities that two molecules would have existed at this point such that first coordination shell of the oxygen atom of water around reference oxygen atom of water at this temperature lies at distance 0.2740 nm.

TABLE II. Detail of RDF $g_{OW-OW}(r)$ at different temperatures.

Temp.	FPP(nm)	FPV	SPP(nm)	SPV	TPP(nm)	TPV	Co-ordination no.
293.20 K	0.2740	3.1514	0.4520	1.1398	0.6880	1.0566	421
303.20 K	0.2760	3.0987	0.4500	1.1176	0.6820	1.0430	406
313.20 K	0.2760	3.0073	0.4500	1.0983	0.6820	1.0395	399
323.20 K	0.2760	2.9360	0.4500	1.0855	0.6900	1.0361	395
333.20 K	0.2760	2.8806	0.4500	1.0778	0.6860	1.0360	393

From table II, we see that when the temperature increases then the peak height decreases, and width of peak increases. This means the solvent becomes less structural. Thermal agitation of atoms on the system also increases with increase in temperature. Up to second decimal, all the respective peak positions are the same for all temperatures.

Co-ordination number is the total no of atoms which are found around the reference atom. In RDF first minima suggests there are possible first co-ordination numbers and this can be calculated by FORTRAN code, then we get first coordination number. The integral equation can be discretized over radial distance as,

$$\sum_{r_i=0}^{r_i=r_o} 4\pi r_i^2 \rho(r) \Delta r. \quad (8)$$

In our case, step size of r (Δr) = 0.002 nm. First coordination numbers are calculated and expressed in table II. It suggests that when the temperature increases with a corresponding decrease in density the coordination number decreases.

From *ffnonbonded.itp* file we see σ for oxygen atom of water is 0.32 nm such that van der Waals radius ($2\frac{1}{2}\sigma$) is approximately 0.36 nm as shown in FIG.4(up). The FPP is less than van der Waals radius– suggests that there are other factors apart from van der Waals interaction.

The shift in the minimum potential energy position of water when Coulomb potential is added to LJ potential is illustrated by the FIG.4(below). Our system incorporates other interactions like bonded and many-body effects, so this minimum position shifts again towards the origin. The minimum potential energy position should lie at the first peak position of the RDF.

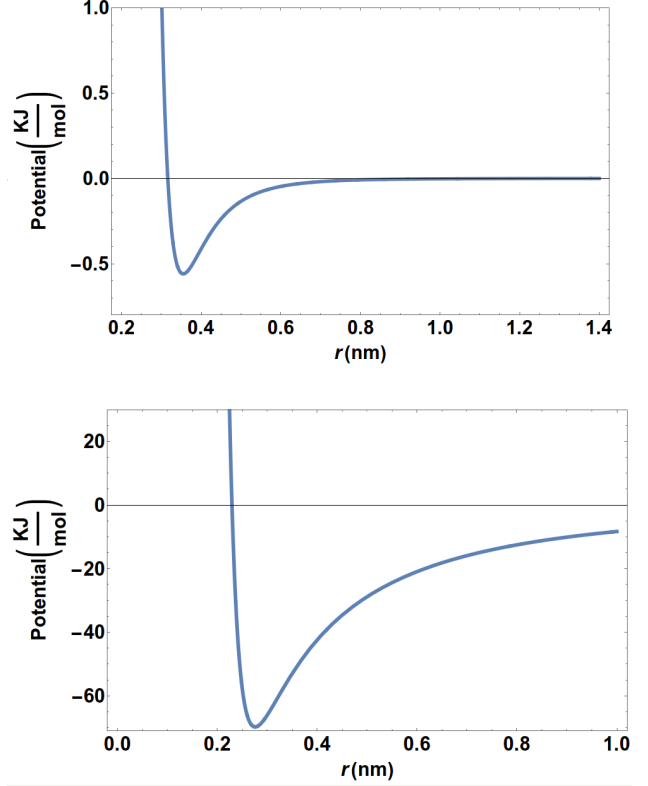


FIG. 4. LJ-(SR)-Potential(up) and LJ-(SR)+Coulomb(SR)-Potential(below) between OW-OW of water at 293.20 K.

Radial Distribution Function of OW-N6

In this system, N6 atom is the nitrogen atom of the amine group of Val and OW is oxygen atom of water: both have negative charge in nature. From the FIG.5 we see that there exists first peak value 1.22 at position 0.28 nm at 293.20 K. It means that there is two or more probability to find oxygen atoms of water around N6 of Val, and radius of first coordination shell of oxygen atom of water around the reference nitrogen atom of Val molecule is FPP of RDF. We can easily see the second peak but the third peak is quite difficult to observe. Both peaks have large width but less height and appear to be 1 after certain distance r , it reflects there is no pair correlation.

Table III represents the details of peak positions, its value and coordination number of FIG.5, we see that when the temperature increases the height of peaks decreases, width increases, and coordination number decreases.

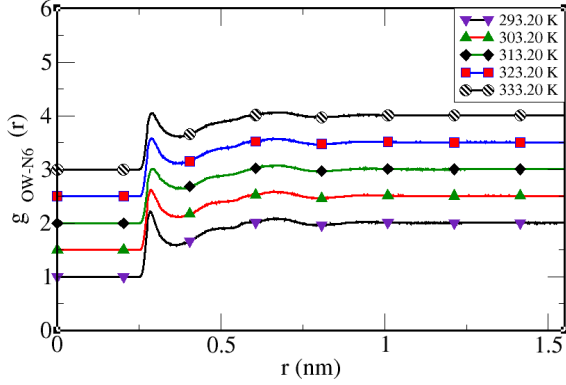


FIG. 5. Plot of the RDF $g_{N6-OW}(r)$ i.e., Nitrogen atoms of Val and Oxygen of water molecules $g(r)$ vs $r(\text{nm})$ at different temperature.

TABLE III. Detail of RDF $g_{N6-OW}(r)$ at different temperatures.

Temp.	FPP(nm)	FPV	SPP(nm)	SPV	TPP(nm)	TPV	Co-ordination no.
293.20 K	0.2840	1.2200	0.6720	1.0860	0.9280	1.0240	113
303.20 K	0.2860	1.1200	0.6620	1.0920	0.9480	1.0230	105
313.20 K	0.2920	1.0090	0.6800	1.0780	0.9560	1.0200	103
323.20 K	0.2880	1.0770	0.6600	1.0740	0.9550	1.0200	101
333.20 K	0.2880	1.0528	0.6840	1.0644	0.9380	1.0193	99

The value of σ for OW-N6 is 0.31 nm. The corresponding van der Waals radius is 0.35 nm. Table III shows that the FPP is less than van der Waals radius—suggests that there are other factors apart from van der Waals interaction like as Coulomb interactions, bonded interactions and many-body effects.

Radial Distribution Function of OW-H19

In this system, H19 is the hydrogen atom which is singled bonded with the oxygen atom of the carboxylic group and OW is oxygen of water molecule. FIG.6 and table IV show that the different peak values and positions. At temperature 293.20 K, FPP is 0.17 nm with corresponding value 2.44, SPP is ≈ 0.38 nm with corresponding value 0.99 and TPP is 0.80 nm with a corresponding value 1.04 after that no peaks appears so there is no pair correlation. The first peak value has the highest among other peaks so in this position, these atoms prefer to remain from each other. FPP is also can be considered as radius of the first coordination shell. We see that when the temperature increases peak value slightly alters and it's width increases this is supposed to due to thermal agitation and bonded or non-bonded interactions.

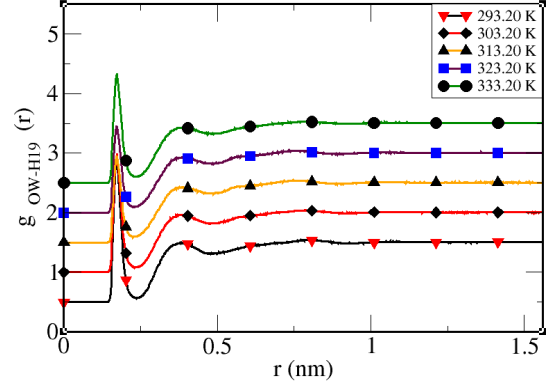


FIG. 6. Plot of the RDF $g_{H19-OW}(r)$ i.e., Oxygen of water and Hydrogen from Carboxylic acid group $g(r)$ vs $r(\text{nm})$ at different temperature.

TABLE IV. Detail of RDF $g_{H19-OW}(r)$ at different temperatures.

Temp.	FPP(nm)	FPV	SPP(nm)	SPV	TPP(nm)	TPV
293.20 K	0.1720	2.4350	0.3780	0.9960	0.8000	1.0430
303.20 K	0.1720	1.9750	0.3960	0.9650	0.7860	1.0410
313.20 K	0.1700	1.4440	0.3870	0.9300	0.7460	1.0420
323.20 K	0.1720	1.8950	0.3880	0.9480	0.7860	1.0370
333.20 K	0.1720	1.8296	0.3920	0.9279	0.7880	1.0321

The value of σ for OW-H19 is 0.00 nm. The corresponding van der Waals radius is 0.00 nm. Table IV shows that the FPP lies at 0.17 nm—suggests that other factors apart from van der Waals interaction like as Coulomb interactions, bonded interactions and many-body effects are highly dominated.

Radial Distribution Function of OW-C1

In our system, C1 is a carbon atom from R-chain of Val molecule. The RDF is taken between C1 and OW. Both have the negative charges but different in magnitude, they have repulsive Coulomb interaction between them. Such that RDF of both are identical. From FIG.7 and table V we can see those different properties as already discussed. At temperature 293.20 K, FPP is ≈ 0.38 nm is a radius of first coordination shell and corresponding value 1.16 means that at this position there is 1.16 times chance to find oxygen atom of water around C1 atom of Val. As in table V, when the temperature increases the peak values decreases, width increases and coordination number decreases. The third peak is difficult to observe but after that, we could not find any observable peak which equals to 1 refers there is no pair correlation beyond this region.

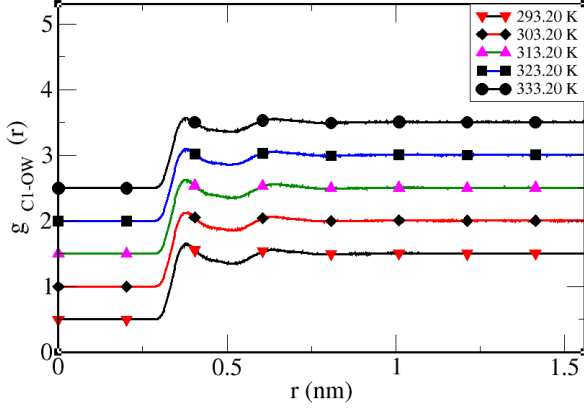


FIG. 7. Plot of the RDF $g_{C1-OW}(r)$ i.e., Oxygen of water and Carbon from R-chain $g(r)$ vs $r(\text{nm})$ at different temperature.

TABLE V. Detail of RDF $g_{C1-OW}(r)$ at different temperatures.

Temp.	FPP(nm)	FPV	SPP(nm)	SPV	TPP(nm)	TPV	Co-ordination no.
293.20 K	0.3780	1.1570	0.6400	1.0670	0.9960	1.0140	437
303.20 K	0.3850	1.1340	0.6360	1.0660	1.0080	1.0160	424
313.20 K	0.3780	1.1280	0.6320	1.0640	1.0640	1.0140	418
323.20 K	0.3760	1.0950	0.6460	1.0590	1.0650	1.0150	397
333.20 K	0.3800	1.0646	0.6380	1.0537	1.0020	1.0146	391

The value of σ for OW-C1 is 0.33 nm. The corresponding van der Waals radius is 0.37 nm. Table V shows that the FPP is less than van der Waals radius—suggests that there are other factors apart from van der Waals interaction like as Coulomb interactions, bonded interactions and many-body effects.

DIFFUSION COEFFICIENTS

Self Diffusion Coefficient of Val

We have estimated self-diffusion coefficient D_{Val}^{Self} of Val at 293.20 K, 303.20 K, 313.20 K, 323.20 K and 333.20 K. FIG.8 shows the MSD vs time of Val for 3 ns and their respective linear fit at different temperatures, It is found that when temperature increases the slope of MSD vs time also increases, such that the self-diffusion coefficient of Val also increases with increase in temperature. It is seen that self-diffusion coefficient of Val at 333.20 K is 120 % greater than at 293.20 K.

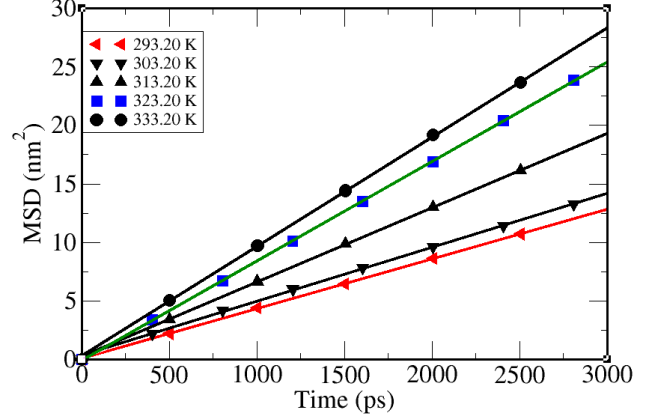


FIG. 8. MSD plots for Val obtained from simulation and their linear fit at different temperatures.

Self Diffusion coefficient of Water

We have estimated self-diffusion coefficient D_{water}^{Self} of water at 293.20 K, 303.20 K, 313.20 K, 323.20 K and 333.20 K. FIG.9 shows the MSD vs time of water for 3 ns and their respective linear fit at different temperatures, It is found that when temperature increases the slope of MSD vs time also increases, such that self-diffusion coefficient of water also increases with increase in temperature. It is seen that self-diffusion coefficient of water at 333.20 K is 111.50 % greater than at 293.20 K.

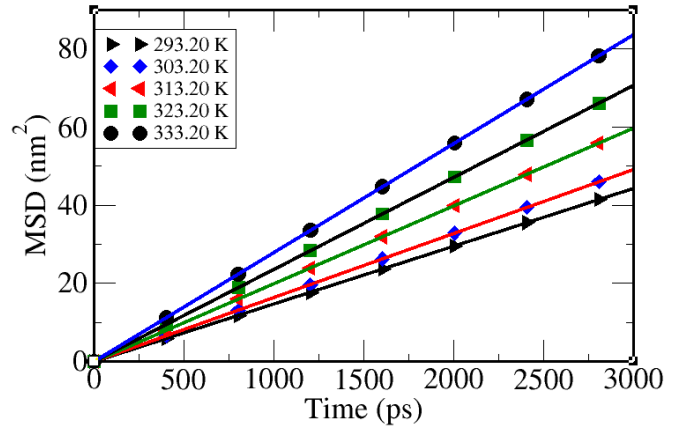


FIG. 9. MSD plot of water at different temperature.

Binary Diffusion Coefficient of Val-water System

During this simulation, we have used 3 Val molecules and 1047 water molecules. Thus, the mole fraction

of Val and water are 0.003 and 0.997 respectively. In this case, Val molecules are very much smaller than water molecules such that the mole fraction of water dominates at all and it's coefficient in equation 2 i.e., D_{Val}^{self} is much closer to the binary-diffusion coefficient.

TABLE VI. Binary - diffusion coefficient of Val in water at different temperatures.

Temp.	Binary-Diffusion (D_{simul}^{binary} in 10^{-10}) m^2/sec	Experimental Value (D_{exp}^{binary} in 10^{-10}) m^2/sec	Error %
293.20 K	7.12 ± 0.30	6.76 ± 0.11	5.32
303.20 K	7.74 ± 0.20	8.91 ± 0.06	13.13
313.20 K	10.65 ± 0.98	11.24 ± 0.10	5.25
323.20 K	14.23 ± 0.89	14.02 ± 0.15	1.50
333.20 K	15.65 ± 0.25	17.03 ± 0.16	8.10

Table VI represents all the simulated values of binary-diffusion coefficient of Val-water mixtures after calculating from Darken's relation at different temperatures. And we compared available experimental result from¹⁵. Our work in simulation is quite close with experimental result spite of being infinite dilution within the error ranging from 1.50 % to 13.13 %.

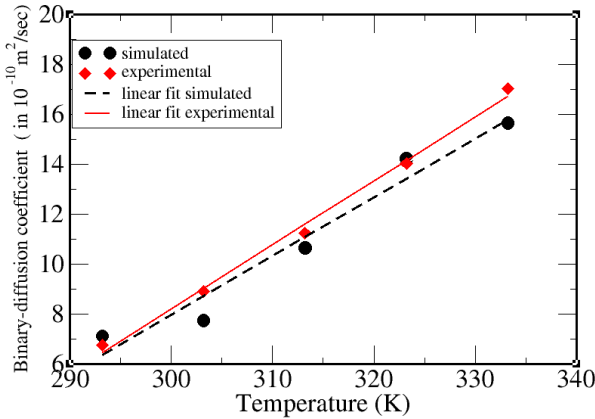


FIG. 10. Variation of the binary-diffusion coefficient with temperature obtained from simulation and experimental literature¹⁵.

In FIG.10, we plotted our simulated result with experimental result found in literature, the black circle points represent our simulated result and diamond square points represent the experimental result. We see that both results are quite close together within some error. From this figure, we can conclude that the binary-diffusion of Val and water increases with increase in temperature.

TEMPERATURE DEPENDENCY OF DIFFUSION

All the graphs and tables of self-diffusion and binary-diffusion show that the diffusion process proportional to the temperature, diffusion increase with an increase in temperature and vice-versa. This relation between temperature and diffusion follow Arrhenius formula⁷.

$$\ln(D) = \ln(D_o) - \frac{E_\alpha}{N_A k_B T} \quad (9)$$

The pre-exponential factor D_o is the frequency factor, E_α is activation energy for diffusion, T is absolute temperature, $N_A = 6.02 \times 10^{23}$ per mol is Avogadro number, and $k_B = 1.38 \times 10^{-23}$ JK⁻¹ is Boltzmann constant. When we plot a graph between natural log (ln) of diffusion coefficient vs reciprocal of absolute temperature is called the Arrhenius diagram. The $-N_A k_B$ times slope of this graph corresponds activation energy of diffusion process which can be expressed as,

$$E_\alpha = -N_A k_B \frac{\partial \ln(D)}{\partial (1/T)} \quad (10)$$

the pre-exponential factor can be obtained when we extrapolate the intercept of this equation to the $1/T \rightarrow 0$.

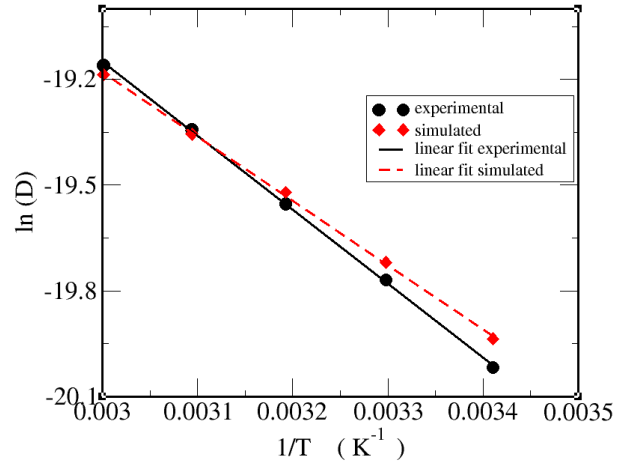


FIG. 11. Arrhenius diagram for the self-diffusion coefficient of water both simulated and experimental.

The FIG.11 is Arrhenius diagram of self-diffusion of water for both simulation and experimental values, corresponding activation energies are 15.14 kJ mol⁻¹ and 17.42 kJ mol⁻¹ respectively. We see that activation energy is in good agreement with the experimental activation energy with error 13.07 %. This is represented in table VII.

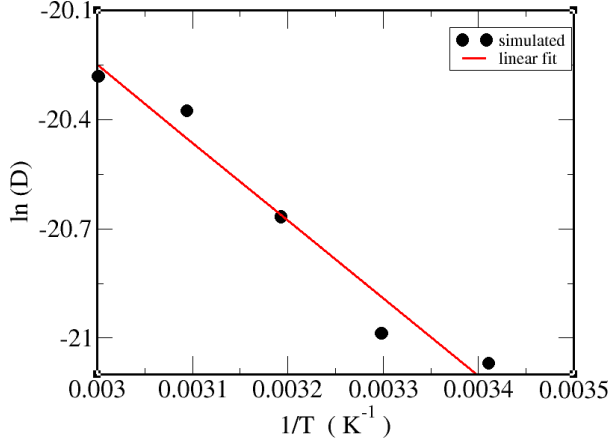


FIG. 12. Arrhenius diagram for the self-diffusion coefficient of Val.

The FIG.12 is Arrhenius diagram of self-diffusion of Val, so activation energy from this diagram for self-diffusion of Val is calculated, which is $17.74 \text{ kJ mol}^{-1}$.

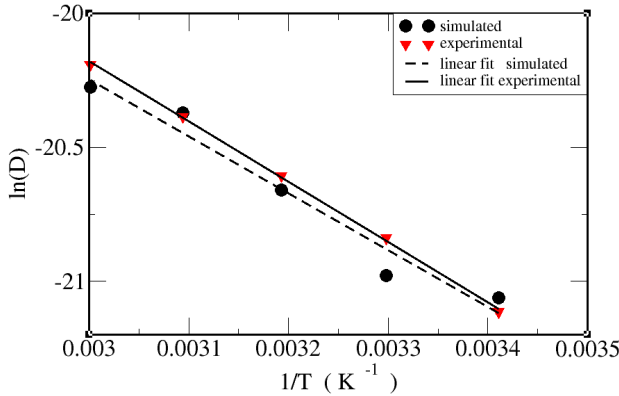


FIG. 13. Arrhenius diagram for the binary-diffusion coefficient of Val-water both simulated and experimental.

The FIG.13 is Arrhenius diagram of binary-diffusion of Val-water for both simulation and experimental values, so activation energies from this diagram are calculated for both case, which are equal to $17.72 \text{ kJ mol}^{-1}$ and $18.72 \text{ kJ mol}^{-1}$ respectively. We see that activation energy is in good agreement with the experimental activation energy with error 5.34 %. Table VII represents activation energies with corresponding species.

TABLE VII. Pre-exponential factor and activation energy of diffusion.

System	Activation energy (E_a) in kJ mol^{-1}		Error Percentage
	Simulated	Experimental	
Water-(self)	15.14	17.42^{24}	13.07
Val-simulated (self)	17.74	—	—
Binary mixture	17.72	18.72^{15}	5.34

CONCLUSIONS AND CONCLUDING REMARKS

We have performed this work under classical molecular dynamics of binary mixture of 1047 water molecules of species SPC/E model and 3 Val molecules at different temperatures 293.20 K, 303.20 K, 313.20 K, 323.20 K, and 333.20 K. The molar concentration was fixed to 0.003 for all the temperatures i.e., almost 160 mol m^{-3} , which was considered as infinite dilution.

We have used GROMACS 4.6.5 package for this simulation in UBUNTU 14.04 environment and we analyzed all the obtained data by XMGRACE and VMD. Bonded interactions like an angle, dihedral were taken into account whereas bond vibration was constrained. All the short-range non-bonded interactions were taken into account and long-range Coulomb interaction was treated by PME and LJ interaction was restricted by cutoff within 1.0 nm. To get the initial minimum energy configuration free from overlaps, energy minimization was done by using the steepest-descent algorithm. This step was found to converge well within the specified tolerance force constant i.e., $50 \text{ kJ mol}^{-1} \text{ nm}^{-1}$. Equilibration was done for 100 ns using NPT ensemble by coupling with velocity rescaling thermostat and Berendsen barostat, which was followed by production run, where production run was simulated for 100 ns using NVT ensemble.

Different energy profiles along with density profiles of the system were studied at different temperatures which were done to know the equilibrium nature of the system. The RDF between different atoms like OW-OW, H19-OW, C1/C3-OW, N6-OW were studied and discussed to know the equilibrium structural properties of the system, Different peaks in RDF allowed to know how atoms were structured in the system, Those peaks helped to analyze the liquid system is more ordered than gases but random to crystalline solid.

The equilibrium dynamical property of the system called the transfer of mass-diffusion coefficient was studied. Concentration gradient was the main factor for diffusion. The self-diffusion coefficient of Val and water at different temperatures were calculated independently by using the MSD method. Then binary diffusion coefficient of Val-water was calculated by using Darken's relation. Both self-diffusion of water and binary diffusion of binary solution were in good agreement with experimental data within error ranging from 1.41 % to 8.54 % and 1.50 % to 13.13 % respectively. The temperature dependence of the diffusion coefficients manifested to follow Arrhenius behavior. Activation energies for different species were calculated from Arrhenius diagram.

This study helps to make the conclusion that molecular

dynamics simulation is one of the best methods to study equilibrium structure and transport properties of biomolecules. Dynamic properties like as diffusion of the binary mixture—which is quite reliable agreement with the experimental result¹⁵. It is economically and computationally less expensive. There are many cases where experimental research is difficult to carry out because of economically expensive. This is quite feasible in our country Nepal where experimental researches are limited due to different cost. For the future study of biomolecules, we can use this calculated diffusion coefficient and structural properties.

In future, we can extend our work in many ways adding transport properties like viscosity and thermal conductivity to our work for different concentrations. Zwitterion of Val at different temperatures and concentrations can be studied. Even allowing long ranged van

der Waals interaction can be another research in the extension of this work, Hard water can be used instead of water. We can study interaction of Val molecules with advanced materials like graphene, carbon nanotube, Nano-bio interactions between carbon nanomaterials and blood plasma proteins is also another field of research.

ACKNOWLEDGEMENTS

D. Pandey acknowledges the financial support from University Grants Commission (UGC), Nepal. NPA also acknowledges UGC Nepal award No. CRG73/74-S&T 01. We also acknowledge the computational facility by ICQ-13.

-
- * npadhikari@tucdp.edu.np
- ¹ A. Panagopoulou, Molecular Dynamics and phase transitions in protein-water system, PhD thesis, National Technical University of Athens faculty of applied mathematics and physics (2013).
 - ² <http://www.aminoacidsguide.com> (2018).
 - ³ <https://pubchem.ncbi.nlm.nih.gov/compound/6287> (2018).
 - ⁴ F. Zhao, and et al., Genetic analysis of pathway regulation for enhancing branched-chain amino acid biosynthesis in plants, *the plant journal*, (1) (2010).
 - ⁵ <https://toxnet.nlm.nih.gov>, L-Valine (2018).
 - ⁶ R.D. Jenert Renne, MS, The amino acid which helps for weight loss, L-Valine, *livestrong.com*, 1(2) (2005).
 - ⁷ M. T. Farran, and O. P. Thomas, Valine Deficiency, the effect of feeding a Valine-Deficient diet during the starter period on performance and leg abnormality of male broiler Chicks1 *Poultry Science*, <http://dx.doi.org/10.3382/ps.0711885> (1992).
 - ⁸ R.B. Russell and M.J. Betts, Amino acid protein and consequences of substitutions in Bioinformatics for Geneticists, publisher=M.R. Barnes, I.C. Gray eds, wiley, <http://www.russelllab.org/aas/Val.html> (2003).
 - ⁹ A. D. Jong and A.C. Borstlap, Transport of amino acids (lvaline, llysine, lglutamic acid) and sucrose into plasma membrane vesicles isolated from cotyledons of developind pea seeds, *Journal of Experimental Botany*, **51**(351) (2000).
 - ¹⁰ D. Allemand, and et al., Characterization of valine transport in sea urchin eggs, *Biochimica et Biophysica Acta (BBA)-Biotechnology Progress*, **772**(3) (1984).
 - ¹¹ J. Kotthaus, and et al., Synthesis and biological evaluation of l-valine-amidoximeesters as double prodrugs of amidines, *Bioorganica & medicinal chemistry*, **19**(6) (2011).
 - ¹² P.L. Smith, and et al., Transport of l-valine-acyclovir via the oligopeptide transporter in the human intestinal cell line, caco-2, *Journal of Pharmacology and Experimental Therapeutics*, **286**(3) (1998).
 - ¹³ M. Ning, and et at., Variation in intestinal transport of l-valine in relation to age, *Experimental Biology and Medicine*, **129**(3) (1968).
 - ¹⁴ Y. Ma, and et at., Studies on the diffusion coefficients of amino acids in aqueous solution, *Journal of Chemical and Engineering Data*, **50**(4) (2005).
 - ¹⁵ T. Umecky, and et al., Infinite dilution binary diffusion coefficients of several α -amino acids in water over a temperature range from (293.2 to 333.2) K with the taylor dispersion technique, *Journal of Chemical & Engineering Data*, **51**(5) (2006).
 - ¹⁶ J. Crank, The mathematics of diffusion, *Oxford university press* (1979).
 - ¹⁷ P. Heitjans and J. Krager, *Diffusion in Condensed Matter; Methods, Materials, Models*, Number 1 Springer (2009).
 - ¹⁸ S. K. Thapa, Molecular dynamics study of diffusion of oxygen in water at different temperatures, Master's thesis, Central Department of Physics, TU Kathmandu Nepal (2010).
 - ¹⁹ L.S. Darken, "Diffusion, Mobility and Their Interrelation through Free Energy in Binary Metallic Systems", *Trans. AIME*, vol. 175, 1 (1948).
 - ²⁰ B. Smit, and et al., *Understanding Molecular simulation from algorithm to apalcaltions*, volume 1, Academic Press, San Diego San Francisco New York Boston London Sydney Tokyo (1996).
 - ²¹ M.P. Allen and D.J. Tildesley. Computer simulation of liquids, volume 18 of oxford science publications, *Oxford University Press*, 45, 121 (1989).
 - ²² B. R. Niraula, Molecular dynamics study of diffusion of propane gas in water at different temperatures, Master's thesis, Central Department of Physics, TU Kathmandu Nepal, Nepal (2017).
 - ²³ D. V. Lindahl, and et al., Gromacs user manual version 4.6, *Search PubMed* (2013).
 - ²⁴ M. Holz, and et al., Temperature-dependent self-diffusion coefficients of water and six selected molecular liquids for calibration in accu-

rate ^1H NMR PFG measurements (2000).